

Flexible and Porous Nonwoven SiCN Ceramic Material via Electrospinning of an Optimized Silazane Solution

Luiz F. B. Ribeiro,* Ricardo S. Cunha, Agenor de Noni Jr, Ricardo A. F. Machado, Günter Motz,* and Sergio Y. G. González*

The processing of nonwoven porous ceramics by combining the polymer-derived ceramic (PDC) route with electrospinning offers an excellent strategy for developing new porous ceramic structures. Currently, the manufacturing of nonwoven porous materials from preceramic polymers is conducted by trial and error approaches. The necessity to predict the e-spinnability conditions from properties assessment offers a potential tool to control the manufacture and the resulting material morphology. This work assesses the relationship between the preceramic polymer solutions and the resulting electrospun nonwoven morphology. For this, a commercially available liquid oligosilazane (Durazane 1800) is selectively cross-linked to achieve a reliable and spinnable preceramic polymer (HTTS), which is then dissolved in tetrahydrofuran (THF). Based on the investigation of the rheological behavior of various polymer concentrations, three different polymer solution regimes (diluted, semidiluted, and concentrated) are identified and correlated with the resulting morphology of the e-spun material (spherical particles, beaded fibers, and seamless fibers). After the pyrolysis, the nonwoven ceramics manufactured from the solution with 65 wt% of HTTS is converted to a SiCN ceramic nonwoven with 86% of open porosity, profiling as a promising candidate for developing high-performance filter systems and catalytic supports in harsh environments.

1. Introduction

One of the essential advantages of the polymer-derived ceramics (PDC) technology is the applicability of well-established polymer processing techniques to manufacture ceramic components in shapes that would not be feasible via conventional powder ceramic techniques. Moreover, manipulating the polymeric precursor chemistry and its molecular architecture allows designing ceramics with tailor-made properties.^[1] The most common precursors (preceramic polymers) are based on silicon-like siloxanes, carbosilanes, and silazanes, leading to the respective oxide or nonoxide ceramics.

Due to the intrinsic properties of silicon-based nonoxide ceramics such as lightweight, high modulus, and excellent chemical and thermal stability, coupled with the versatility of being shaped in a wide variety of forms, PDCs can be potentially applied in several key areas related to energy, environment, transport, and defense.^[1,2] Like other materials, by increasing the surface area of PDC components,

its performance is improved for several applications, especially those related to catalytic supports and filtration. Suitable for such applications are especially cellular materials (synergy of high surface area and the inherent properties of the ceramics)^[3] and structures based on nanofibers, e.g., processed by combining the PDC route with electrospinning.^[4]


The obtained 1D nanostructure arranged in the form of mats possesses a large surface-to-volume ratio, which, combined with the aforementioned intrinsic properties of PDCs, makes these components excellent candidates for high-performance filtering systems and also as catalytic supports in harsh environments.^[5–9] In addition, the ceramic mats can be modified or functionalized to extend their application in areas such as electrochemical devices.^[10–16] Finally, the use of electrospun PDCs, in combination with different nanostructures, has been explored as promising candidates for electromagnetic wave absorption, as seen in recent literature.^[17–22]

Despite several advantages, the literature on electrospun PDCs is still scarce, and the electrospinning requirements of the preceramic polymers are not fully understood yet. The main challenge is to meet the needed properties for electrospinning.^[23,24]

L. F. B. Ribeiro
Graduate Program in Energy and Sustainability
Federal University of Santa Catarina
Araçuaí 88906-072, Brazil
E-mail: luiz.ribeiro@ufsc.br

R. S. Cunha, A. de Noni, Jr, R. A. F. Machado, S. Y. G. González
Graduate Program in Chemical Engineering
Federal University of Santa Catarina
Florianópolis 88010-970, Brazil
E-mail: sergio.gomez@ufsc.br

G. Motz
Department of Ceramic Materials Engineering
University of Bayreuth
Bayreuth D-95447, Germany
E-mail: guenter.motz@uni-bayreuth.de

 The ORCID identification number(s) for the author(s) of this article can be found under <https://doi.org/10.1002/adem.202100321>.

© 2021 The Authors. Advanced Engineering Materials published by Wiley-VCH GmbH. This is an open access article under the terms of the Creative Commons Attribution License, which permits use, distribution and reproduction in any medium, provided the original work is properly cited.

DOI: 10.1002/adem.202100321

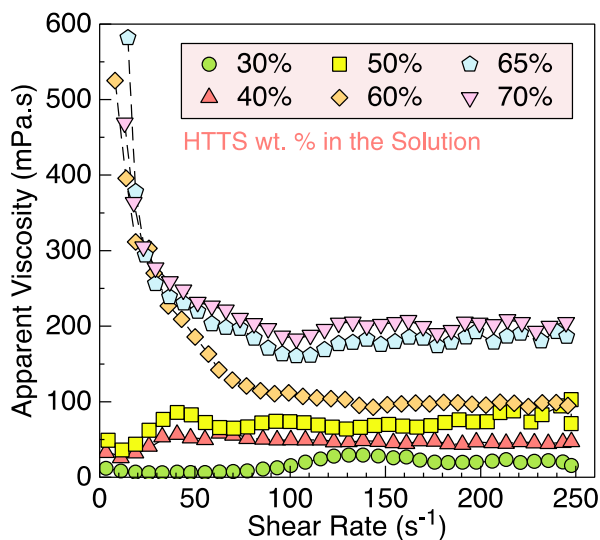


Figure 2. Dependency of the viscosity from the shear rate for HTTS solutions with different concentrations.

polymer chains gradually start to interact through chain entanglement by increasing the polymer concentration. This change from diluted to semidiluted state allows the formation of fibers, instead of beaded fibers or even droplets during electrospinning.^[23,27]

As the polymer concentration is increased to more than 65 wt%, a second transition point occurs, characterized by a remarkable increase in the viscosity. This phenomenon is better visualized by plotting the mean viscosities at the plateau regime (η_{∞}) as a function of the polymer concentration (Figure 3).

As will be further discussed in the e-spinning experiments section, this transition leads to seamless fibers, as an increase in the solution concentration leads to a higher degree of polymer chain entanglements.^[26,27]

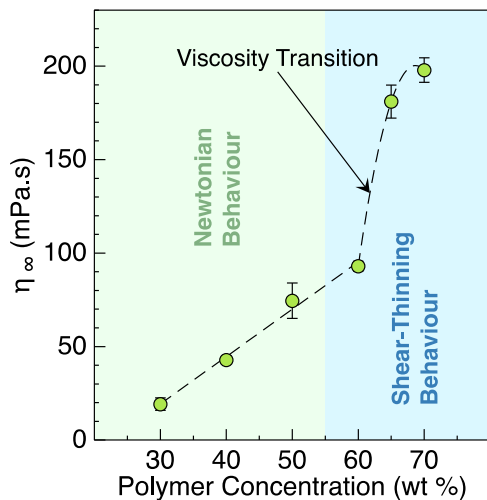


Figure 3. Dependence of viscosity of HTTS solutions with different concentrations at steady state.

2.3. Manufacturing of Pre-ceramic Polymer Fibers by e-Spinning

The e-spinning process with the HTTS solutions was performed as described in the experimental procedure. The respective spinning results are shown in Figure 4.

Figure 4 clearly shows the strong influence of the HTTS concentration, i.e., the solution viscosity on the morphology of the resulting materials. As predicted by the rheological behavior, the e-spinning of the diluted solutions ranging from 30 to 50 wt% of HTTS yields only near-spherical polymer particles, as the Taylor cone formation was not possible. The Taylor cone formation is a precondition for the processing of regular-shaped fibers via the e-spinning process.^[28,29] Thus, the polymer solutions were directly ejected from the needle tip in the form of a spray jet. For this interval of concentration, the term e-spraying should be more appropriate to describe this processing scenario. In summary, for diluted solutions, the lack of chain entanglements avoids the drawn jet continuity and leads only to the deposition of small droplets at the collector.

Particles with a mean diameter size of 7.8 ± 2.6 , 8.4 ± 2.0 , and $9.4 \pm 1.4 \mu\text{m}$ were obtained from samples HTTS_1, HTTS_2, and HTTS_3, respectively. It is worth mentioning that the increase in polymer concentration also leads to the formation of more homogeneous particles with a narrower size (Figure 4 and 5). However, in addition to particles, the formation of small fibrils was observed for sample HTTS_3, which is in agreement with the rheological results and confirms the beginning of the transition to a semidiluted regime.

The increase in the polymer concentration to 60 wt% (sample HTTS_4) leads to the formation of beaded fibers. This morphology results from two types of instability during the e-spinning process, the Rayleigh and varicose instabilities,^[30–33] which favor spheres formation because of the smallest surface area to diminish the surface tension. In the sample with 65 wt% HTTS concentration (HTTS_5), the viscosity seems to have inhibited beads-on-string fiber formation, leading to seamless fibers. Increasing the HTTS concentration in the solution to 70 wt% (HTTS_6), the high viscosity combined with the low solvent concentration leads to nonhomogeneous tape-like morphology with a broader size distribution, here named as flat-scattered fibers. For better visualization, the measured average fiber diameters are shown in Figure 5.

2.4. Investigation of the Pyrolysis Behavior and NonWoven Ceramic Formation

The pyrolysis of organosilazanes up to $1000 \text{ }^{\circ}\text{C}$ in N_2 leads to the formation of an amorphous ceramic composed of a $\text{SiC}_x\text{N}_{4-x}$ ($0 \leq x \leq 4$) matrix and a segregated carbon phase (so-called free carbon).^[34–37] For ceramic fibers processed through pyrolysis, the crosslinking step is crucial to convert the thermoplastic pre-ceramic polymer to a thermoset, avoiding shape changes during the ceramization.^[38] For this purpose, considering the availability of vinyl groups in HTTS, a radical initiator (AIBN) was used to perform the cross-linking step. Figure 6 shows the resulting fibers pyrolyzed as described in the experimental procedure.

After pyrolysis, defect-free cylindrical SiCN fibers with a diameter $<4 \mu\text{m}$ were obtained, which is far below the reported diameter for the same ceramic fibers processed by melt spinning

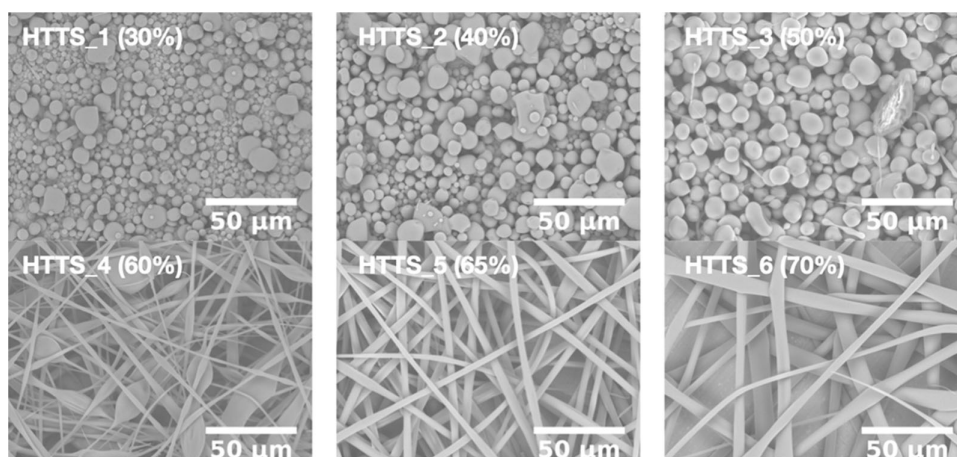


Figure 4. Scanning electron microscopy (SEM) micrographs of the formed particles and fibers during e-spinning in dependency on the HTTS solution concentration.

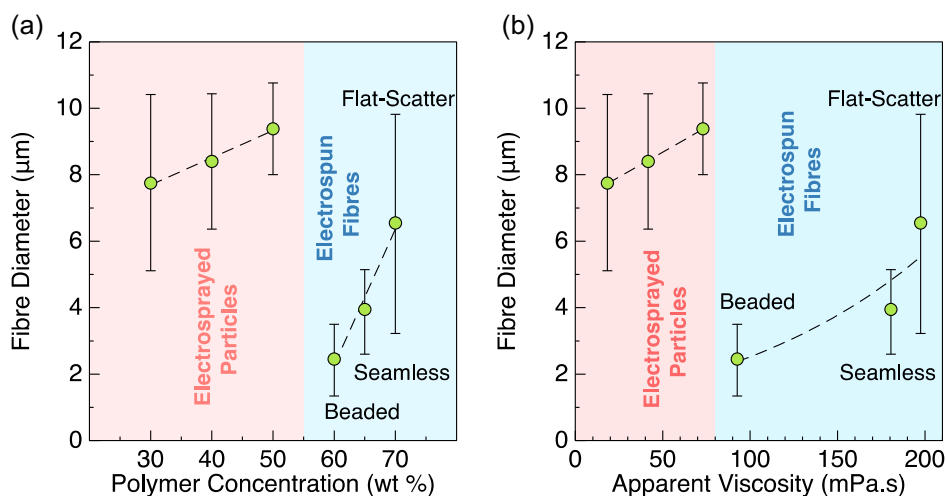


Figure 5. Dependence of polymer morphology and average diameter on the a) polymer concentration and b) viscosity.

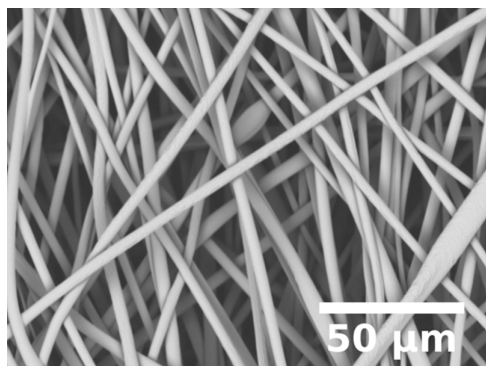


Figure 6. SEM micrographs of HTTS₅-derived e-spun fibers pyrolyzed at 1000 °C in N₂ atmosphere.

(30–100 μm)^[25] and also lower than commercially available SiC fibers (≈10 μm).^[39] Although the fabricated fibers are still in the

range of micrometers, their quality in terms of homogeneity and morphology is remarkable, as no additional organic polymer (spinning aid) was used. The decomposition gases derived from organic additives would evolve during pyrolysis, which could lead to defects and a higher shrinkage, both very deleterious for the fiber properties. Further optimization of the e-spinning process should lead to fibers with a diameter in the range of nanometers.

Another essential characteristic of the PDCs technology is the significant shrinkage during the pyrolysis, mainly assigned by the remarkable increase in density and the mass loss during the conversion from a polymer to ceramics. The fiber average diameter and the nonwoven dimensions were used to estimate the shrinkage for sample HTTS₅ during pyrolysis (**Figure 7**).

Comparing the fiber diameter before and after pyrolysis, a shrinkage of 22% is noticed, as the fiber mean diameter decreases from 4.1 μm (before pyrolysis) to 3.2 μm (after pyrolysis). The shrinkage is one of the drawbacks of the PDCs technology, and this phenomenon must be considered for further product designing. Regarding the ceramic nonwoven porosity,

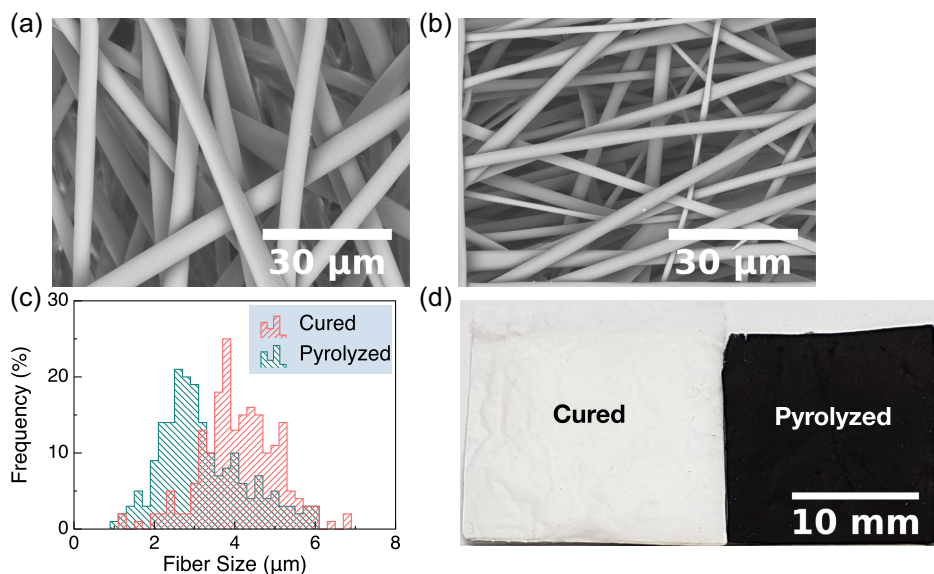


Figure 7. SEM micrographs of HTTS_5-derived e-spun fibers a) before and b) after pyrolysis. c) Histogram of polymer and ceramic fiber diameter distribution, and d) nonwoven porous material comparison before and after pyrolysis.

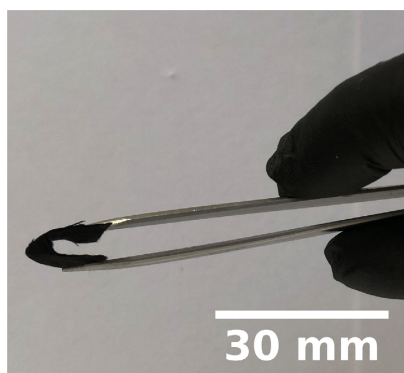


Figure 8. Flexibility demonstration of HTTS_5-derived e-spun nonwoven after pyrolysis.

the percentage of total porosity was estimated at approximately 86%. The calculation was performed as described in the experimental section by considering the measured SiCN ceramic true density ($\rho_T = 2.416 \text{ g cm}^{-3}$) and the calculated nonwoven density ($\rho_A = 0.347 \text{ g cm}^{-3}$). Finally, it is noteworthy to mention that because of the thin ceramic fibers the porous nonwoven ceramic is flexible and presents sufficient mechanical strength to be bent and handled without breaking or losing its structural integrity (**Figure 8**). The good mechanical properties, the well-known thermal and chemical stability, and the good shapeability open many promising applications, such as in filtering systems, catalyst supports, and porous burners.

3. Conclusions

Many preceramic polymers have a much lower molecular weight compared with organic polymers. Therefore, it is crucial to add

organic polymers as spinning aid to enable processing via electrospinning. However, such organic additives act as sacrificial filler, which leads to a decreased ceramic yield, higher shrinkage, and the formation of pores within the formed ceramic fibers during pyrolysis and results in inferior mechanical properties. The approach developed here overcomes these problems.

In this work, solutions of the polysilazane HTTS in THF, synthesized by selective cross-linking of the oligosilazane Durazane 1800, were specially designed and comprehensively investigated for the electrospinning process. The rheological measurements of different feedstock solutions were correlated with the resulting fiber morphology after electrospinning, to predict the morphology of the e-spun preceramic polymers. For diluted solutions with a polymer concentration lower than 50 wt%, only near-spherical particles with diameters in the range of 7–10 μm were obtained, as no interactions of the polymer chains are present. By increasing the polymer concentration up to 60 wt%, the HTTS solution rheology reveals a shear-thinning behavior, indicating the transition to a semidiluted state due to a certain degree of chain entanglements. Fibers with beads-on-string morphology are typical for this solution regime. For concentrations higher than 65 wt%, the substantial increase in the viscosity and a viscoelastic behavior due to a higher degree of chain entanglements lead to seamless fibers during the electrospinning process.

The pyrolysis behavior was investigated for samples with a concentration of 65 wt% of HTTS containing AIBN as curing agent. The pyrolysis led to defect-free ceramic SiCN fibers with a diameter $< 4 \mu\text{m}$. Due to the resulting thin diameter, the porous ceramic nonwoven possesses excellent flexibility. Finally, the ceramic nonwoven porous structure indicates a total porosity of about 86%.

The developed approach enables the electrospinning of preceramic polymers without e-spinning aids and helps to conduct this process methodically. Further improvements of the electrospinning process combined with the functionalization of the

ceramics should lead to specially tailored morphology, structure, and properties. The results achieved open promising PDC technology applications as filter systems and catalytic supports intended for harsh environments.

4. Experimental Section

Materials: The commercially available oligosilazane Durazane 1800 (Merck KGaA, Germany) was selected as the SiCN precursor. Tetra-*n*-butylammonium fluoride (TBAF) (1 M in THF) was used as the catalyst, while calcium borohydride bis(tetrahydrofuran) (Ca(BH₄)₂·2THF) was used as an inhibitor to stop the reaction, both purchased from Sigma Aldrich (Germany). THF p.a. (Neon, Brazil) was used for the synthesis and the e-spinning experiments, and the initiator 2,2'-azobisisobutyronitrile (AIBN), used for curing, was supplied by Akzo Nobel (The Netherlands). The educts' preparation and handling and all synthesis reactions were conducted in a dry argon atmosphere.

Selective Cross-Linking of the Oligosilazane: The procedure adopted to perform the selective chemical cross-linking of the oligosilazane Durazane 1800 based on a previous work reported by Flores et al.^[25] In a typical reaction, 20 g of Durazane 1800 was dissolved under vigorous stirring in 40 g of THF, and 0.25 wt% of the catalyst TBAF, concerning Durazane 1800, was added dropwise to the reaction. The solution was stirred for 90 min, and an excess of the inhibitor (Ca(BH₄)₂·2THF) was added to stop the reaction. The mixture was stirred for another 5 min and afterward filtered off. Finally, the solvent was removed under reduced pressure at room temperature, obtaining a solid and colorless polysilazane, hereafter called HTTS.

E-Spinning Experiments and Pyrolysis: Solutions varying from 30 to 70 wt% of HTTS in THF were prepared for the electrospinning experiments. The respective solution was placed in a 5 mL syringe coupled with a metallic needle of 0.7 mm inner diameter clamped to a high-voltage power supply applying 10 kV and fixed at 10 cm from an aluminum collector. The sample was extruded at a flow rate of 1 mL h⁻¹ controlled by an infusion syringe pump arranged horizontally.

For the pyrolysis, 1.5 wt% of the curing agent AIBN, referred to HTTS amount, was added to the spinning solution. Then, the resulting polymer nonwoven was cured at 70 °C for 4 h to enable cross-linking before melting. Afterward, the sample was placed in a carbon crucible and heated up to 1000 °C (2 K min⁻¹) under nitrogen flow in a tubular furnace.

Rheological Characterization: Parallel plate rotational rheology of the polymer solutions was performed in a Thermo Scientific Haake Mars II rheometer (Thermo Fisher Scientific, USA) using a PP60 measuring geometry (60 mm diameter). A 0.15 gap was used in the tests, and the shear rate varied from 0.1 to 250 s⁻¹ in 60 s. All measurements were performed at a temperature of 23 ± 1 °C.

Fiber Morphology Investigation: The e-spun samples were analyzed to assess the fiber morphology before and after the pyrolysis by scanning electron microscopy TM3030 (Hitachi, Japan), operating at an acceleration voltage of 15 kV. The micrographs obtained were analyzed by the ImageJ software (National Institutes of Health, USA), and 200 measurements for either fibers or particles were used to estimate the reported mean values.

Investigations of the NonWoven Properties: The ceramic nonwoven porosity (ϵ) was estimated by using **Equation 1**

$$\epsilon = 1 - \frac{\rho_A}{\rho_T} \quad (1)$$

where ρ_A is the nonwoven apparent density and ρ_T is the true density of the derived SiCN material. For the apparent density, the volume was obtained by measuring the nonwoven dimensions, while for the true density, the ceramic volume was determined with a gas pycnometer (Accu Pyc II 1340 – Micromeritics Instruments Corporation, USA).

Acknowledgements

The authors like to thank CAPES (Coordenação de Aperfeiçoamento de Pessoal de Nível Superior) within the project PROBRAL (88881.198816/2018-01) and DAAD (German Academic Exchange Service, Project-ID 57446974) for financial support.

Open access funding enabled and organized by Projekt DEAL.

Conflict of Interest

The authors declare no conflict of interest.

Data Availability Statement

The data that support the findings of this study are available from the corresponding author upon reasonable request.

Keywords

electrospinning, nonwoven ceramics, polymer-derived ceramics, porous ceramics, SiCN, silazanes

Received: March 17, 2021

Revised: June 8, 2021

Published online: July 22, 2021

- [1] P. Colombo, G. Mera, R. Riedel, G. D. Sorarù, *J. Am. Ceram. Soc.* **2010**, *93*, 1805.
- [2] G. Mera, M. Gallei, S. Bernard, E. Ionescu, *Nanomaterials* **2015**, *5*, 468.
- [3] C. Vakifahmetoglu, D. Zeydanli, P. Colombo, *Mater. Sci. Eng. R Rep.* **2016**, *106*, 1.
- [4] A. Viard, P. Miele, S. Bernard, *J. Ceram. Soc. Jpn.* **2016**, *124*, 967.
- [5] S. Xie, Y. Wang, Y. Lei, B. Wang, N. Wu, Y. Gou, D. Fang, *RSC Adv.* **2015**, *5*, 64911.
- [6] B. Wang, Y. Wang, Y. Lei, N. Wu, Y. Gou, C. Han, *Mater. Manuf. Process.* **2016**, *31*, 1357.
- [7] W. Nan, W. Lynn Yuqin, W. Ying-De, F. KO, *J. Inorg. Mater.* **2018**, *33*, 357.
- [8] S. H. Koo, S. G. Lee, H. Bong, Y.-J. Kwark, K. Cho, H. S. Lim, J. H. Cho, *Polymer (Guildf)*. **2014**, *55*, 2661.
- [9] A. Guo, M. Roso, M. Modesti, J. Liu, P. Colombo, *J. Appl. Polym. Sci.* **2014**, *131*.
- [10] A. Tolosa, M. Widmaier, B. Krüner, J. M. Griffin, V. Presser, *Sustain. Energy Fuels* **2018**, *2*, 215.
- [11] S. A. Smith, B. P. Williams, Y. L. Joo, *J. Membr. Sci.* **2017**, *526*, 315.
- [12] S. A. Smith, J. H. Park, B. P. Williams, Y. L. Joo, *J. Mater. Sci.* **2017**, *52*, 3657.
- [13] Z. Sang, X. Yan, L. Wen, D. Su, Z. Zhao, Y. Liu, H. Ji, J. Liang, S. X. Dou, *Energy Storage Mater.* **2020**, *25*, 876.
- [14] Q. Chen, D. Jia, B. Liang, Z. Yang, Y. Zhou, D. Li, R. Riedel, T. Zhang, C. Gao, *Ceram. Int.* **2021**, *47*, 10958.
- [15] S. Bin Mujib, R. Cuccato, S. Mukherjee, G. Franchin, P. Colombo, G. Singh, *Ceram. Int.* **2020**, *46*, 3565.
- [16] M. Ma, H. Wang, X. Li, K. Peng, L. Xiong, X. Du, *J. Eur. Ceram. Soc.* **2020**, *40*, 5238.
- [17] Y. Huo, Y. Tan, K. Zhao, Z. Lu, L. Zhong, Y. Tang, *Chem. Phys. Lett.* **2021**, *763*, 138230.
- [18] F. Xiao, H. Sun, J. Li, X. Guo, H. Zhang, J. Lu, Z. Pan, J. Xu, *Ceram. Int.* **2020**, *46*, 12773.

- [19] X. Guo, F. Xiao, J. Li, H. Zhang, Q. Hu, G. Li, H. Sun, *Ceram. Int.* **2021**, 47, 1184.
- [20] Y. Zhang, Y. Zhao, Q. Chen, Y. Hou, Q. Zhang, L. Cheng, L. Zheng, *Ceram. Int.* **2021**, 47, 8123.
- [21] Y. Huo, K. Zhao, Z. Xu, Y. Tang, *J. Alloys Compd.* **2020**, 815, 152458.
- [22] Y. Hou, L. Cheng, Y. Zhang, X. Du, Y. Zhao, Z. Yang, *Chem. Eng. J.* **2021**, 404, 126521.
- [23] M. G. McKee, G. L. Wilkes, R. H. Colby, T. E. Long, *Macromolecules* **2004**, 37, 1760.
- [24] R. Rošic, J. Pelipenko, P. Kocbek, S. Baumgartner, M. Bešter-Rogač, J. Kristl, *Eur. Polym. J.* **2012**, 48, 1374.
- [25] O. Flores, T. Schmalz, W. Krenkel, L. Heymann, G. Motz, *J. Mater. Chem. A* **2013**, 1, 15406.
- [26] S. K. Tiwari, S. S. Venkatraman, *Mater. Sci. Eng. C* **2012**, 32, 1037.
- [27] S. L. Shenoy, W. D. Bates, H. L. Frisch, G. E. Wnek, *Polymer (Guildf)*. **2005**, 46, 3372.
- [28] T. Subbiah, G. S. Bhat, R. W. Tock, S. Parameswaran, S. S. Ramkumar, *J. Appl. Polym. Sci.* **2005**, 96, 557.
- [29] G. Taylor, *Proc. R. Soc. London. Ser. A Math. Phys. Sci.* **1964**, 280, 383.
- [30] M. M. Hohman, M. Shin, G. Rutledge, M. P. Brenner, *Phys. Fluids* **2001**, 13, 2201.
- [31] W. Zuo, M. Zhu, W. Yang, H. Yu, Y. Chen, Y. Zhang, *Polym. Eng. Sci.* **2005**, 45, 704.
- [32] J. H. Yu, S. V. Fridrikh, G. C. Rutledge, *Polymer (Guildf)*. **2006**, 47, 4789.
- [33] H. Zhao, H. Chi, in *Nov. Asp. Nanofibers*, (Eds: T. Lin) IntechOpen, London, England **2018**, p. 13, Ch. 5.
- [34] S. Traßl, D. Suttor, G. Motz, E. Rössler, G. Ziegler, *J. Eur. Ceram. Soc.* **2000**, 20, 215.
- [35] G. Ziegler, H.-J. Kleebe, G. Motz, H. Müller, S. Traßl, W. Weibelzahl, *Mater. Chem. Phys.* **1999**, 61, 55.
- [36] J. Seitz, J. Bill, N. Eggerb, F. Aldinger, *J. Eur. Ceram. Soc.* **1996**, 16, 885.
- [37] C. Gérardin, F. Taulelle, D. Bahloul, *J. Mater. Chem.* **1997**, 7, 117.
- [38] G. Motz, S. Schmidt, S. Beyer, in *Ceramic Matrix Composites*. (Ed: Walter Krenkel), Wiley-VCH Verlag GmbH & Co. KGaA, Weinheim, Germany **2008**, p. 165.
- [39] O. Flores, R. K. Bordia, D. Nestler, W. Krenkel, G. Motz, *Adv. Eng. Mater.* **2014**, 16, 621.